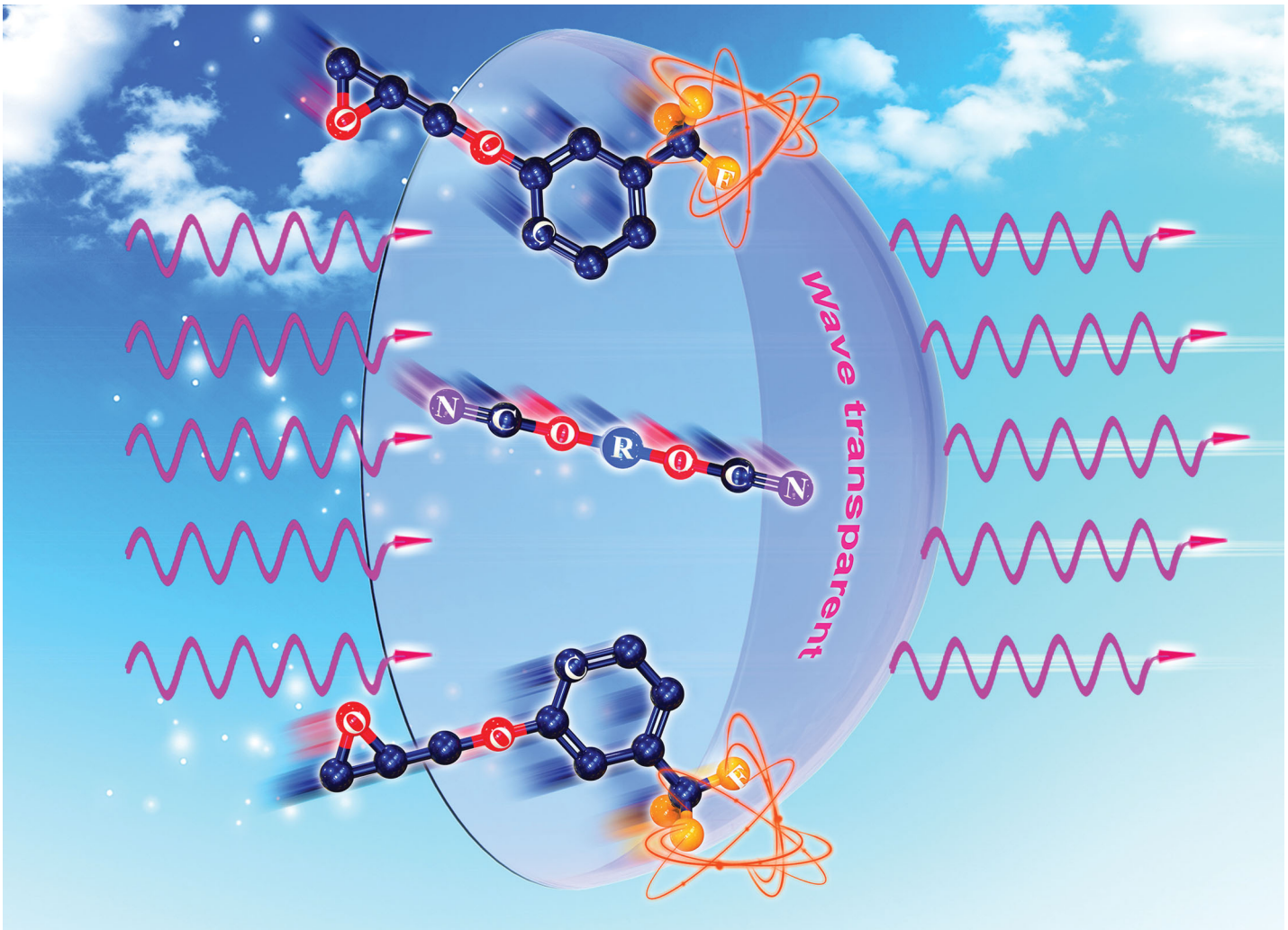

Showcasing research from the School of Science at Northwestern Polytechnical University and the Integrated Composites Lab at the University of Tennessee.

Ultralow dielectric, fluoride-containing cyanate ester resins with improved mechanical properties and high thermal and dimensional stabilities

A new preparation strategy for fluoride-containing compounds modified with cyanate ester resins was presented giving rise to ultra-low dielectric properties, prominent mechanical properties and excellent thermal & dimensional stabilities.

As featured in:

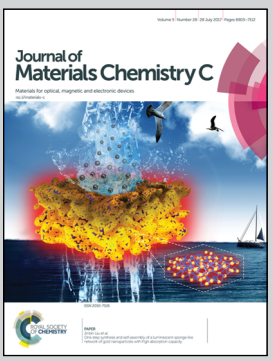

See Jie Kong, Zhanhu Guo *et al.*, *J. Mater. Chem. C*, 2017, **5**, 6929.

ROYAL SOCIETY OF CHEMISTRY

rsc.li/materials-c

Registered charity number: 207890

Journal of Materials Chemistry C

PAPER

View Article Online
View Journal | View Issue

Cite this: J. Mater. Chem. C, 2017, 5, 6929

Ultralow dielectric, fluoride-containing cyanate ester resins with improved mechanical properties and high thermal and dimensional stabilities

Junwei Gu,[a] Wencai Dong,[a] Yusheng Tang,[a] Yongqiang Guo,[a] Lin Tang,[a] Jie Kong,*[a] Sruthi Tadakamalla,[b] Bin Wang[c] and Zhanhu Guo*[b]

Received 14th January 2017,
Accepted 10th May 2017

DOI: 10.1039/c7tc00222j

rsc.li/materials-c

In this contribution, we present a new strategy for the fabrication of modified cyanate ester resins combined with ultralow dielectric properties, improved mechanical properties and high thermal and dimensional stabilities. The fluoride-containing compound 2-((3-(trifluoromethyl)phenoxy)methyl)oxirane (TFMPMO), synthesized from *m*-(trifluoromethyl)phenol (TFMP) and epichlorohydrin (ECH), was used to modify bisphenol A dicyanate ester (BADCy) resins *via* copolymerization reaction. The BADCy resin modified with 15 wt% TFMPMO presented ultralow dielectric constant (ε, 2.75) and dielectric loss tangent values ($\tan\delta$, 6.7 $\times$ 10^{-3}), high mechanical properties (impact strength of 15.4 kJ m^{-2} and flexural strength of 141.0 MPa), and superior thermal and dimensional stability ($T_{\text{Heat-resistance index}}$ of 206 °C and coefficient of thermal expansion of 6.4 $\times$ 10^{-5}), and it possesses great potential application in radomes and antenna systems of aircraft.

1. Introduction

Cyanate ester (CE) resins have demonstrated many unique properties such as high temperature resistance, easy processability, ultralow dielectric constant (ε of 2.6–3.2) and dielectric loss ($\tan\delta$ of 0.005–0.010) values and relatively good stability in a wide range of temperatures and electric field frequencies in comparison to bismaleimide (BMI), polyimide (PI) or epoxy resin (EP).[1–6] At the same time, CE resins possess good mechanical properties, good heat and humidity resistance, low water adsorption, preferable flame retardancy and dimensional stability, and they could have wide applications in the fields of sensing,[7] packaging,[8] aerospace and microelectronics, especially for radomes and satellite antenna systems.[9–12] Especially, compared to other thermosets (BMI, PI, EP, *etc.*), CE presents relatively lower ε and $\tan\delta$ values.[13–16] However, a big gap facing its application in high-performance radomes is the narrow wave bands of pure CE matrix. Therefore, the fabrication and modification of CE matrix with low dielectric properties have received increasing interest in recent years.

The blend and copolymerization modification methods are normally performed to reduce the ε and $\tan\delta$ values of CE matrix. For example, Zhuo *et al.* fabricated hollow silicate tube/CE blends, and the corresponding ε and $\tan\delta$ values were reduced to 2.7 and 9.2 $\times$ 10^{-3}, respectively.[17] Zhang *et al.* adopted amino-functionalized polyhedral oligomeric silsesquioxane (NH_2-POSS) to modify CE matrix, and the ε and $\tan\delta$ values were decreased to 2.9 and 3.6 $\times$ 10^{-3}, respectively.[18] Hu *et al.* prepared modified CE resin by synthesizing hyperbranched maleimide containing polysiloxane, and the ε and $\tan\delta$ values were reduced to 3.0 and 6.0 $\times$ 10^{-3}, respectively.[19] Shieh *et al.* synthesized multiple monofunctional CE resins to modify CE resins *via* copolymerization, and the minimum ε and $\tan\delta$ values were 2.3 and 8.6 $\times$ 10^{-3}, respectively.[20,21] However, the corresponding mechanical properties and the thermal and dimensional stabilities of the above CE modifiers were often inevitably decreased, and thus, the existing modified CE resins still cannot satisfy the requirements of high-performance radomes.

Fluoropolymers possess outstanding heat resistance, high chemical and aging resistance, extremely low friction coefficient and high flame retardancy,[22,23] and they have been widely applied in the fields of microelectronics, biomedicine and aerospace, *etc.*[24–27] Fluoropolymers also present ultralow ε and $\tan\delta$ values owing to their larger free volume, small dipole and low polarization of C–F bonds.[28–31] Their use has proven to be a viable way to fabricate relatively low-dielectric-constant materials by introducing fluoride-containing groups into the main chains or side chains of polymers. For example, Zhou *et al.* fabricated

[a] Key Laboratory of Space Applied Physics and Chemistry, Ministry of Education, Department of Applied Chemistry, School of Science, Northwestern Polytechnical University, Xi'an, Shaanxi, 710072, P. R. China. E-mail: kongjie@nwpu.edu.cn
[b] Integrated Composites Laboratory (ICL), Department of Chemical & Biomolecular Engineering, University of Tennessee, Knoxville, TN 37996, USA. E-mail: zguo10@utk.edu
[c] Engineered Multifunctional Composites (EMC) Nanotech LLC, Knoxville, TN 37934, USA

low-dielectric-constant phenolic resins by introducing fluoride-containing groups, and both the ε and tan δ values were reduced to 2.5 and 3.1 $\times$ 10^{-3}, respectively.[32] Tao *et al.* reported that the ε and tan δ values of the fluoride-containing epoxy resin were reduced by 11.1% and 69.6% in comparison to those of pure epoxy resins.[33,34] The modified epoxy resin with C–F bonds by Wang *et al.* also presented a dramatic reduction in ε and tan δ values (2.0 and 4.4 $\times$ 10^{-2}).[35] However, to the best of our knowledge, the copolymerization modification of CE matrix *via* fluoride-containing epoxy groups to reduce the dielectric constant while retaining other physical and chemical properties of the CE matrix has not yet been reported.

In this work, we present a new strategy for the fabrication of modified cyanate ester resins combining ultralow dielectric properties, improved mechanical properties and high thermal and dimensional stabilities. Epoxy groups were firstly introduced to the fluoride-containing compounds, which were copolymerized with CE matrix to prepare the corresponding fluoride-containing CE resins. Herein, the fluoride-containing compounds of 2-((3-(trifluoromethyl)phenoxy)methyl)oxirane (TFMPMO) were firstly synthesized from *m*-(trifluoromethyl)phenol (TFMP)[36] and epichlorohydrin (ECH). The molecular structure of the TFMPMO was characterized by ^{1}H nuclear magnetic resonance (^{1}H NMR) spectroscopy and Fourier transform infrared (FTIR) spectroscopy. The obtained fluoride-containing TFMPMO was used to prepare novel ultralow-dielectric-constant, TFMPMO-modified bisphenol A dicyanate ester (BADCy) resins *via* copolymerization reaction. The effects of the TFMPMO content on the dielectric properties, mechanical properties, and thermal and dimensional stabilities of the TFMPMO-modified BADCy resins were investigated in detail.

2. Experimental

2.1. Materials

Bisphenol A dicyanate ester (BADCy) resins, with a density of 1.171 g cm^{-3} and molecular weight of 278.31, were received from Jiangsu Wuqiao Resin Factory Co., Ltd, China. *m*-(Trifluoromethyl)phenol (TFMP) was obtained from Aladdin Reagent Co., Ltd, China. Epichlorohydrin (ECH) was purchased from TCI Development Co., Ltd, Japan. Dichloromethane was obtained from Tianjin Chemical Reagent Co., Ltd, China. Potassium carbonate was received from Kermel Chemical Reagent Co., Ltd, China. Di-*n*-butyltin dilaurate was supplied by Alfa Aesar Chemical Co., Ltd, China. All the materials were used as received without any further treatment.

2.2. Synthesis of 2-((3-(trifluoromethyl)phenoxy)methyl)oxirane (TFMPMO)

m-(Trifluoromethyl)phenol (16.20 g, 0.10 mol) and potassium carbonate (16.60 g, 0.12 mol) were added into a three-necked flask with a reflux condenser and a mechanical stirrer, in which the reaction was firstly maintained at 120 °C for 30 min.[37] ECH (46.26 g, 0.50 mol) was then added into the flask and stirred for another 4 h. The obtained mixture was then extracted by distilled water and dichloromethane, followed by rotary evaporation and chromatography, and the corresponding product TFMPMO was finally obtained (Scheme 1).

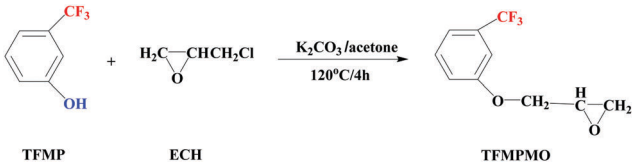

Scheme 1 Schematic diagram of the synthesis route of TFMPMO.

2.3. Fabrication of the TFMPMO-modified BADCy resins

BADCy resins were firstly heated to 150 °C and stirred magnetically for a certain time. Then, a certain quantity of TFMPMO was added into the above BADCy and stirred uniformly. The mixture was degassed in a vacuum oven, then poured into the preheated mold at 150 °C. It was then cured according to the provided procedures[16] of 180 °C/2 h + 200 °C/6 h, followed by post-curing in a vacuum oven at 220 °C/2 h. The reaction mechanism of TFMPMO and BADCy is shown in Scheme 2.

2.4. Characterizations

The ^{1}H nuclear magnetic resonance (^{1}H NMR) spectra of the samples were measured on a Bruker Avance 400 MHz system (Bruker Bio Spin, Switzerland) to determine the molecular structure, with $CDCl_3$ as a solvent and tetramethylsilane (TMS) as an internal standard. Fourier transform infrared (FTIR) spectra of the samples were obtained on Bruker Tensor 27 equipment (Bruker Co., Germany) with thin films on KBr. Scanning electron microscope (SEM) morphologies of the samples were observed using a VEGA3-LMH (TESCAN Corporation, Czech Republic). Thermal gravimetric analyses (TGA) of the samples were carried out using STA 449F3 (Netzsch C Corp., Germany) at

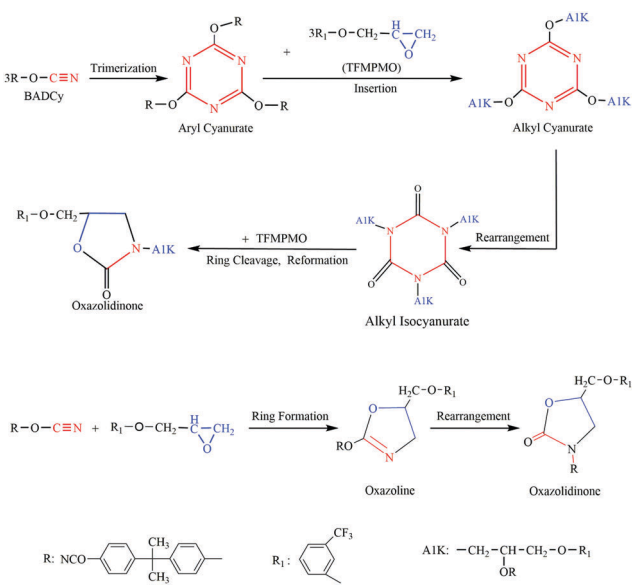

Scheme 2 The reaction mechanism of the TFMPMO and BADCy matrix.

10 °C min^{-1} (argon atmosphere), over the entire temperature range (40–900 °C). The coefficient of thermal expansion (CTE) values of the samples were measured on the DIL402C (Netzsch, Germany) with a heating rate of 2 °C min^{-1} over the entire temperature range of 25–150 °C. The dimension of the specimens was 25 mm × 10 mm × 4 mm. The dielectric constant (ε) and dielectric loss factor (tan δ) values of the samples were measured using a Novocontrol Technologies Alpha-N high-resolution dielectric analyzer (Novocontrol, Germany) at room temperature.[35] The dimension of the specimens was 10 mm × 10 mm × 1.3 mm.

The flexural strength values of the samples were measured using an Electron Omnipotence Experiment Machine SANS2CMT5105 (Shenzhen New Sansi Corp., China) according to the standard ISO178-1993. The impact strength values of the samples were measured with a XCJ-40 impact testing machine (Chengde Materials Testing Corp., China) according to the standard ISO 179-1993.

3. Results and discussion

3.1. Structural analysis of the TFMPMO

Fig. 1 shows the ^{1}H NMR spectra of the ECH (a), TFMP (b) and TFMPMO (c). For the protons in methylene connecting with chlorine, the corresponding chemical shift is changed from 3.6 ppm (Fig. 1(a)) to 4.0 ppm and 4.3 ppm (Fig. 1(c)). Meanwhile, the chemical shift of phenolic hydroxyl at 5.3 ppm (Fig. 1(b)) disappears in Fig. 1(c), ascribed to the alkylation reaction between ECH and TFMP. In addition, the chemical shift for each proton in Fig. 1(c) is a one-to-one correspondence to that of TFMPMO, and the corresponding integration area of the peaks is in agreement with that of TFMPMO, proving that the TFMPMO has been synthesized by alkylation reaction between ECH and TFMP.

The FTIR spectra of TFMP and TFMPMO are presented in Fig. 2. The bands around 1675–1500 cm^{-1} can be assigned to the stretching vibration peak of benzene ring. The stretching vibration peaks at 3360 and 1350–1120 cm^{-1} can be attributed to the phenolic hydroxyl and –CF_3, respectively. For TFMPMO, the phenolic hydroxyl peak at 3360 cm^{-1} disappears, and the corresponding characteristic absorption peaks near 3000 cm^{-1} (methylene) and 910 cm^{-1} (epoxy group) are observed. The results demonstrate that TFMPMO has been synthesized.

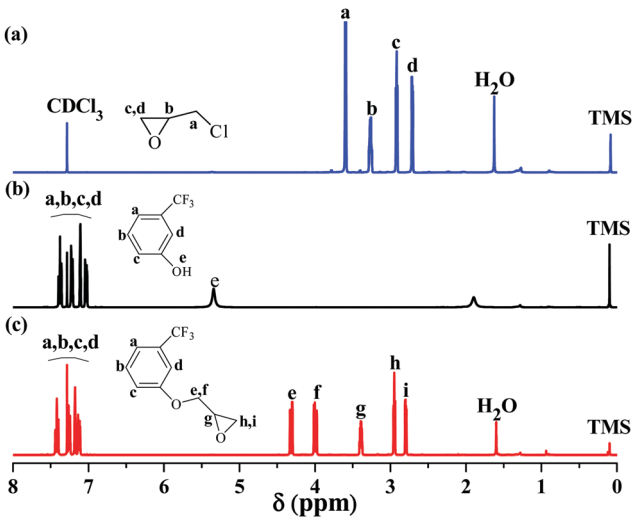

Fig. 1 The ^{1}H-NMR spectra of the (a) ECH, (b) TFMP, and (c) TFMPMO.

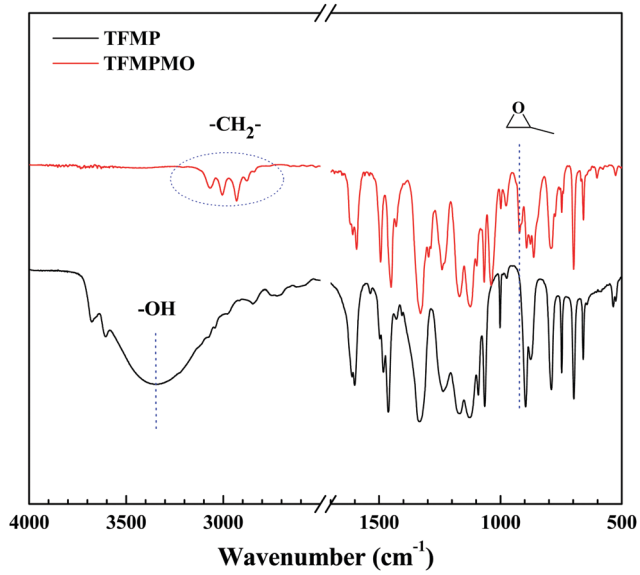

Fig. 2 FTIR spectra of TFMP and TFMPMO.

3.2. On-line FTIR spectra of TFMPMO-modified BADCy resins

Fig. 3 shows the on-line FTIR spectra of pure BADCy and TFMPMO-modified BADCy resins. The bands near 2275 and 2238 cm^{-1} can be ascribed to the stretching vibration of the –OCN group. After curing at 180 °C for 2 h, the stretching vibration peak of the –OCN group is significantly weakened, and the characteristic stretching vibration peaks at 1566 and 1370 cm^{-1} of the triazine also appear. As the curing reaction further progresses, the stretching vibration peaks of the –OCN group are gradually weaken and disappear. The stretching vibration peaks of triazine are strengthened, ascribed to the complete curing reaction of BADCy. Compared to that of pure BADCy, the new characteristic absorption peak at 1645 cm^{-1} of oxazoline also appears in the TFMPMO-modified BADCy resins (Fig. 3b), owing to the copolymerization reaction between TFMPMO and BADCy.

3.3. Dielectric properties of the TFMPMO-modified BADCy resins

Fig. 4 shows the effects of the TFMPMO content on the ε and tan δ values of the TFMPMO-modified BADCy resins at different frequencies. Both ε and tan δ values of the TFMPMO-modified BADCy resins decreased with the addition of TFMPMO. For the same loading of TFMPMO, the corresponding ε and tan δ values are decreased slightly with increasing the frequency. The TFMPMO-modified BADCy resin with 15 wt% TFMPMO possesses optimal dielectric properties, *i.e.*, ε of 2.75 and tan δ of 6.7 × 10^{-3} at 10 MHz, are reduced by 8.3% and 17.3%,

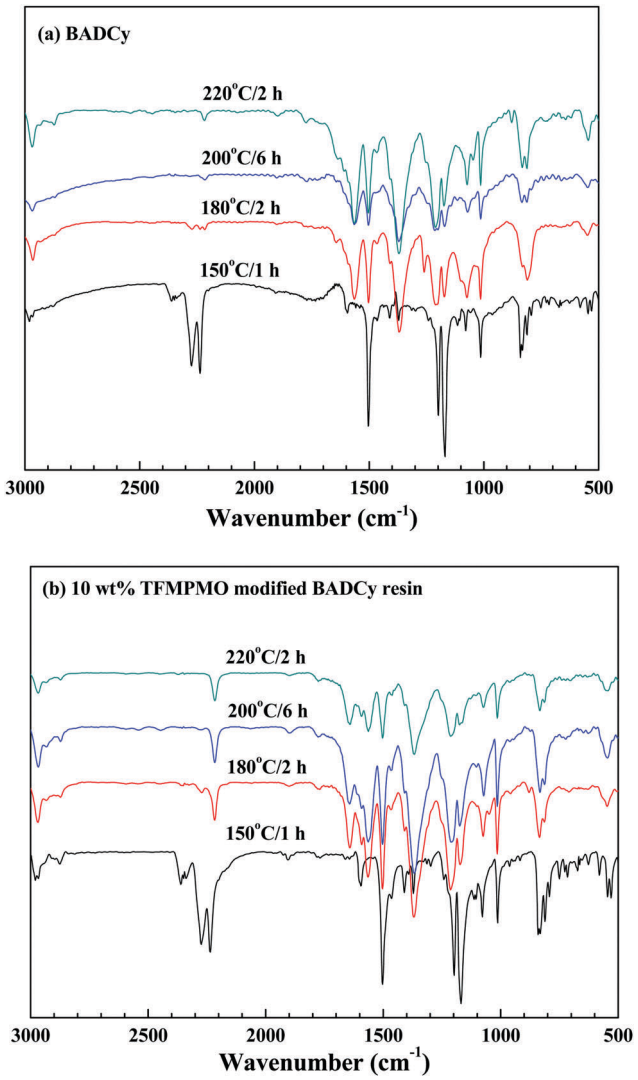

Fig. 3 On-line FTIR spectra of (a) pure BADCy and (b) TFMPMO-modified BADCy resins.

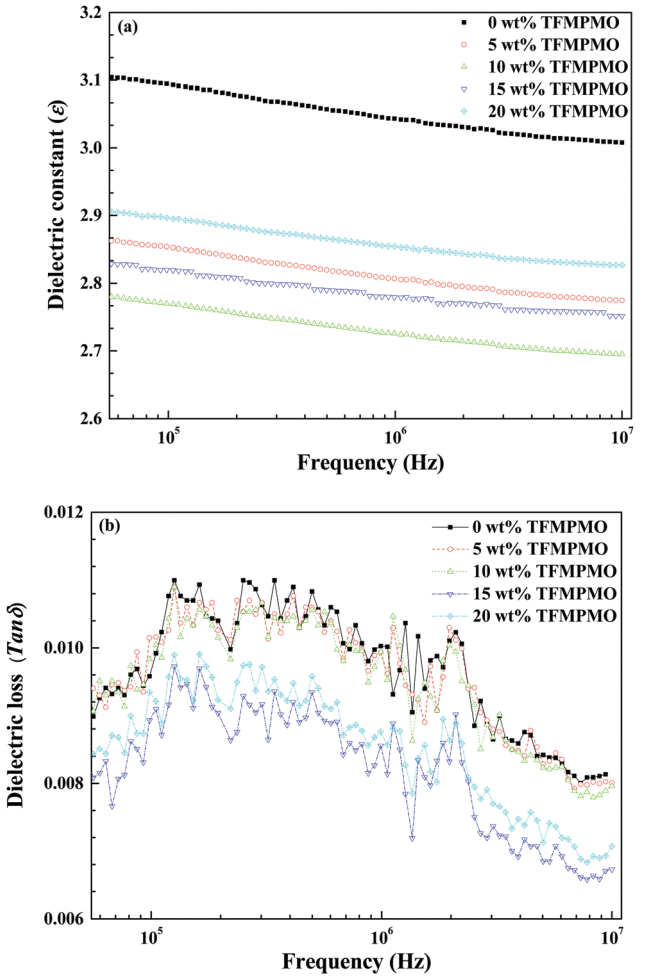

Fig. 4 The effects of TFMPMO contents on the ε (a) and tan δ (b) values of the TFMPMO-modified BADCy resins at different frequencies.

respectively, compared to that of pure BADCy (ε of 3.0 and tan δ of 8.1 $\times$ 10^{-3}).

On one hand, the $-CF_3$ group possesses large free volume, the C–F bond presents a low polarization, and the F atom can reduce electronic polarizability, in favor of decreasing ε and tan δ values of the TFMPMO-modified BADCy resins. On the other hand, the epoxy groups in TFMPMO can react with the –OCN groups in BADCy to form oxazoline with a large polarization, resulting in the increase of ε and tan δ values. The role of both aspects would determine the final ε and tan δ values. In addition, with increasing the frequency (Debye dispersion equation[38]), the response of polar groups can never keep up with the changes of alternating electric field to reduce the orientation polarization, in favor of further decreasing the ε and tan δ values of the TFMPMO-modified BADCy resins.

Herein, the internal polarizability of the BADCy mainly includes electronic polarizability, ionic polarizability and dipolar polarizability. According to the Debye dispersion equation,[38] the corresponding ε and tan δ are expressed as eqn (1) and (2), respectively:

$$\varepsilon' = \varepsilon_\infty + \frac{\varepsilon_s - \varepsilon_\infty}{1 + \omega^2\tau^2} \quad (1)$$

$$\tan\delta = \frac{(\varepsilon_s - \varepsilon_\infty)\omega\tau}{\varepsilon_s + \omega^2\tau^2\varepsilon_\infty} \quad (2)$$

where ω represents the frequency; τ represents the relaxation time; ε_∞ represents optical dielectric constant (ω close to zero); and ε_s represents the static dielectric constant (ω close to infinity).

From eqn (1), the corresponding ε value decreases with increasing ω value. The reason is that different polarization modes require different amounts of time. Polarization in the lower region does not work when the changing frequency of electric field exceeds a certain limitation. Therefore, the ε value decreases with increasing the frequency. Additionally, for $\omega\tau = \sqrt{\frac{\varepsilon_s}{\varepsilon_\infty}}$, the tan δ value is the maximum. The reason is that with increasing the ω value, the correlative polarization cannot

keep up with the change of electric field, resulting in the increase of tan δ value. Moreover, with increasing the frequency at the higher frequency region, some polarization components will not be sensitive to the changing frequency, thus resulting in the decrease of tan δ value.[39] Based on the density functional theory (DFT), the structure of TFMPMO was optimized by the method of M062X with 6-311G (d, p), and the calculation result of intrinsic vibration frequency for TFMPMO was 9.5×10^{11}–9.7×10^{13} Hz (31.7–3235.9 cm^{-1}), which was far above the maximum frequency (2×10^6 Hz) of the applied electric field frequency in our experiments. For orientation polarization, the polar molecules need to overcome their own inertia and rotation resistance in the external electric field, which requires a longer amount of time. The corresponding orientation frequency is in the range of 10^3–10^8 Hz,[39] which may not keep up with the external electric field of the experiments.

In addition, the mechanism of the dielectric properties is discussed as follows. The dielectric constant can be correlated with polarizability of molecules by using the Clausius–Mosotti equation as shown in eqn (3):[40]

$$\varepsilon = 1 + \frac{3N\alpha}{3\varepsilon_0 - N\alpha} \quad (3)$$

where N represents the number of molecules per unit dielectric volume; α represents the polarizability (electronic polarizability, ionic polarizability, dipolar polarizability and real charge polarizability); and ε_0 represents the vacuum permittivity. From eqn (3), it could be deduced that ε has a monotonously increasing relationship with the molecule density and polarizability. Therefore, the smaller the N and α were, the smaller the ε. In our work, with the introduction of F groups, 2s and 2d of F atom could decrease the electronic effects from the external electric field, thus decreasing the polarizability (α) of BADCy.

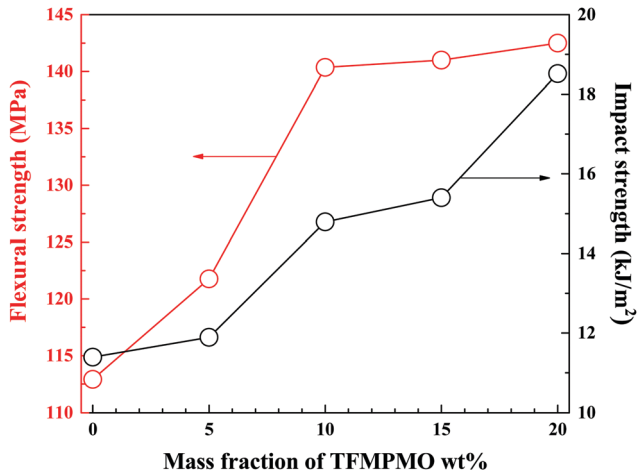

Fig. 5 The effects of TFMPMO content on the mechanical properties of the TFMPMO-modified BADCy resins.

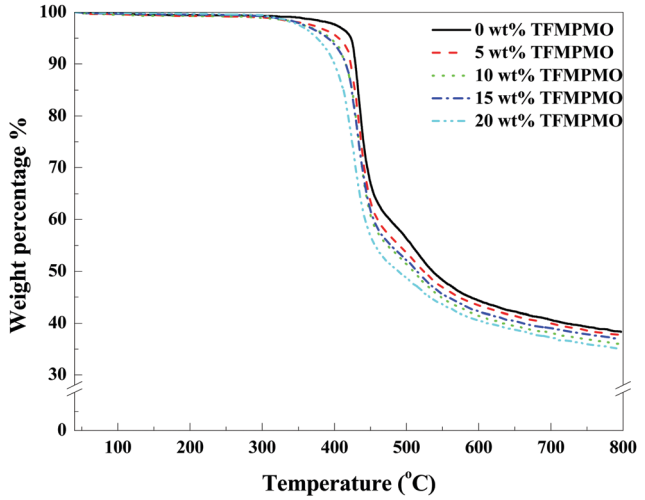

Fig. 7 TGA curves of the TFMPMO-modified BADCy resins.

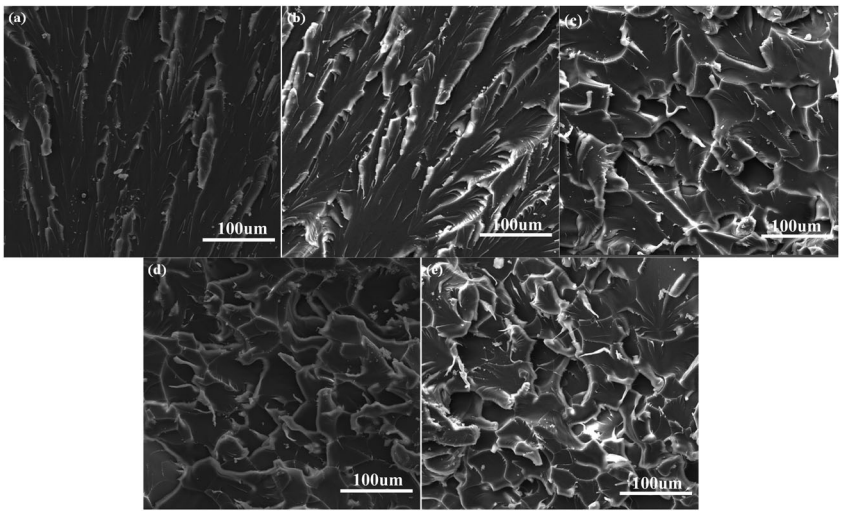

Fig. 6 SEM morphologies of impact fractures for the TFMPMO-modified BADCy resins with a TFMPMO content of (a) 0, (b) 5, (c) 10, (d) 15 and (e) 20 wt%.

Table 1 Characteristic thermal data of BADCy and the TFMPMO-modified BADCy resins

Samples	Weight loss temperature/°C			
	T_5	T_{30}	T_{50}	$T_{\text{Heat-resistance index}}$[a]/°C
Pure BADCy	422.9	445.6	536.1	213.9
5 wt% TFMPMO/BADCy	405.9	441.4	523.6	209.3
10 wt% TFMPMO/BADCy	394.2	438.3	509.1	206.1
15 wt% TFMPMO/BADCy	390.8	438.6	514.6	205.5
20 wt% TFMPMO/BADCy	376.0	429.4	488.8	199.9

[a] The sample's heat-resistance index is calculated by eqn (4)

$$T_{\text{Heat-resistance index}} = 0.49 \times [T_5 + 0.6 \times (T_{30} - T_5)] \quad (4)$$

where T_5 and T_{30} are the corresponding decomposition temperature of 5% and 30% weight loss, respectively.

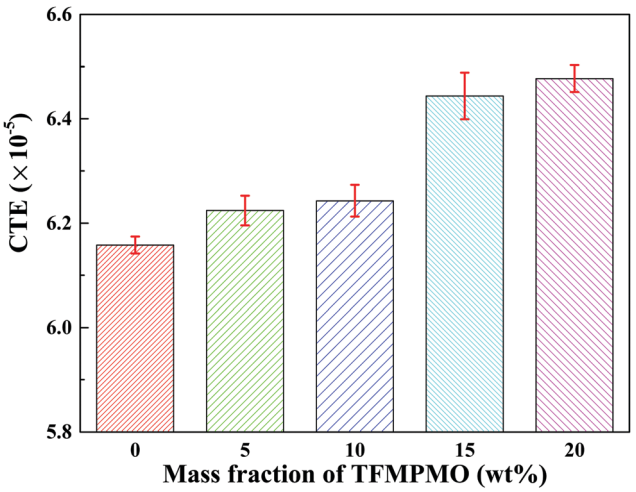

Fig. 8 The influence of TFMPMO content on the CTE values of the TFMPMO-modified BADCy resins.

On the other hand, the larger free volume of F groups could decrease the number of polar molecules per unit volume (N).[28–31,41] Therefore, the modified BADCy presented better dielectric properties.

3.4. Mechanical properties of the TFMPMO-modified BADCy resins

Fig. 5 shows the influence of TFMPMO content on the mechanical properties of the TFMPMO-modified BADCy resins. Both the impact and flexural strength of the TFMPMO-modified BADCy resins are gradually increased with the addition of increasing amounts of TFMPMO. Compared with those of BADCy (impact strength for 11.4 kJ m^{-2} and flexural strength of 112.9 MPa), the maximum impact and flexural strength of the TFMPMO modified BADCy resins are improved to 18.5 kJ m^{-2} and 142.5 MPa, increased by 62.3% and 26.2%, respectively. The reason is that the $-CF_3$ group in the TFMPMO possesses large free volume, in favor of increasing the chain flexibility of BADCy, thus enhancing impact strength. Moreover, oxazoline can replace partly rigid triazine structures, which is beneficial to the improvement of the flexural and impact strength for the TFMPMO-modified BADCy resins.

Fig. 6 shows the SEM morphologies of impact fractures for the TFMPMO-modified BADCy resins. The impact fracture surface of pure BADCy is observed to be relatively smooth, presenting a typical brittle feature. With 5 wt% TFMPMO, the impact fracture surface presents a typical river-like morphology. The introduction of TFMPMO can transfer stress, restrain the propagation of cracks and consume energy, thereby improving the impact strength of the TFMPMO-modified BADCy resins. With further addition of the TFMPMO, stress whitening can be clearly seen, and the degree of stress whitening is also increased with increasing TFMPMO content. The reason is that plenty of micro-crack accumulation areas in the TFMPMO-modified BADCy resins are generated under stress. These can absorb and consume some of the energy, which is beneficial for enhancing the impact toughness.

3.5. Thermal properties of the TFMPMO-modified BADCy resins

Fig. 7 shows the TGA curves of the TFMPMO-modified BADCy resins, and the corresponding characteristic thermal data are summarized in Table 1. The corresponding $T_{\text{Heat-resistance index}}$ (T_{HRI})[42] values of the TFMPMO-modified BADCy resins decreased with

Table 2 The comprehensive properties of the pure BADCy, modified BADCy and epoxy resins

Samples		Dielectric properties		Mechanical properties		Thermal properties
		ε	$\tan\delta$ ($\times10^{-3}$)	Flexural strength (MPa)	Impact strength (kJ m^{-2})	Carbon yields (%)
Pure BADCy		3.0	8.1	112.9	11.4	40.6
Modified BADCy	Our present work (TFMPMO)	2.75	6.7	142.5	18.5	39.0
	Polysiloxane@polyimide core–shell microsphere[43]	3.13	7.5	120.0	25.0	30.0
	Poly(urea-formaldehyde) microcapsules with epoxy[44]	4.1	5.0	—	—	44.0
	Octa(aminopropyl)silsesquioxane (POSS-NH_2)[18]	2.91	2.6	—	—	—
	Poly(urea-formaldehyde) microcapsules filled with dibutyltin dilaurate catalyst (PUF/DBTDL MCs)[45]	2.95	3.5	98	9.6	—
	Phenolic resin containing diphenyl oxide segments[46]	3.0	6.2	—	11.9	39.3
	Maleimide-functionalized hyperbranched polysiloxane[19]	3.03	6.0	—	7.2	—
	Methyl silsesquioxane (Me-SSQ)[47]	2.76	6.0	70.0	6.0	—
	4-*tert*-Butylphenol cyanate ester (4TPCY)[48]	2.73	5.4	—	—	43.7
	Epoxy resin[49]	3.7	19.0	97.0	—	17.6

increasing the TFMPMO content. This reveals that the addition of the TFMPMO is against the heat resistance of the TFMPMO-modified BADCy resins. The corresponding T_{HRI} value of the TFMPMO-modified BADCy resin with 20 wt% TFMPMO is 200 °C, still showing relatively high thermal stability. The reason is that the intrinsic heat resistance of the TFMPMO is relatively poorer in comparison to that of pure BADCy, and oxazoline also has a relatively worse heat resistance than triazine, resulting in decreased thermal stabilities.

Fig. 8 presents the influence of TFMPMO content on the coefficient of thermal expansion (CTE) values of the TFMPMO-modified BADCy resins. The CTE values of the TFMPMO-modified BADCy resins increased slightly with increasing the TFMPMO content. The corresponding CTE value of the TFMPMO-modified BADCy resins with 20 wt% TFMPMO is near 6.5×10^{-5}, slightly higher than that of pure BADCy resin (6.2×10^{-5}). Compared to pure BADCy, TFMPMO possesses relatively poorer heat resistance. Furthermore, the addition of TFMPMO can destroy the crosslinked network of the triazine and decrease the cross-linking density of the TFMPMO-modified BADCy resins. The decreased cross-linking density results in the decrease of the thermal and dimensional stabilities.

Comparisons with other studies have been conducted as shown in Table 2. From the comparison, the modified BADCy resins with 15 wt% TFMPMO present the optimal comprehensive properties (ultralow dielectric properties, high mechanical properties and excellent thermal and dimensional stabilities).

4. Conclusions

The synthesized TFMPMO can react with BADCy to produce oxazoline. Both the ε and $\tan\delta$ values of the TFMPMO-modified BADCy resins decreased with the addition of TFMPMO. For the same loading of TFMPMO, the ε and $\tan\delta$ values decreased slightly with increasing the frequency. With increased addition of TFMPMO, the mechanical properties (impact and flexural strength) of the TFMPMO-modified BADCy resins gradually increased, the corresponding weight loss temperatures and T_{HRI} values slightly decreased, and the CTE values increased as well. The modified BADCy resins with 15 wt% TFMPMO present low ε and $\tan\delta$ value, improved mechanical properties, and high thermal and dimensional stability, *i.e.*, ε of 2.75, $\tan\delta$ of 6.7×10^{-3}, impact and flexural strength of 15.4 kJ m^{-2} and 141.0 MPa, T_{HRI} of 206 °C and CTE of 6.4×10^{-5}.

Acknowledgements

The authors are grateful for the support and funding provided by the National Natural Science Foundation of China (No. 51403175), financial support from the Foundation of Aeronautics Science Fund (2015ZF53074 and 2015ZF53071), Seed Foundation of Innovation and Creation for Graduate Students in Northwestern Polytechnical University, and Undergraduate Innovation Program in Northwestern Polytechnical University (201510699256 and 201610699271). Z. Guo appreciates the American Chemical Society Petroleum Research Fund (ACS PRF#: 53930-ND6).

References

1 B. Wang, L. Liu, G. Liang, L. Yuan and A. Gu, *J. Mater. Chem. A.*, 2015, **3**, 23162–23169.
2 M. Zhang, H. Yan, L. Yuan and C. Liu, *RSC Adv.*, 2016, **6**, 38887–38896.
3 (*a*) J. Gu, W. Dong, S. Xu, T. Tang, L. Ye and J. Kong, *Compos. Sci. Technol.*, 2017, **144**, 185–192; (*b*) H. Gu, C. Ma, C. Liang, X. Meng, J. Gu and Z. Guo, *J. Mater. Chem. C*, 2017, **5**, 4275–4285; (*c*) J. Gu, S. Xu, Q. Zhuang, Y. Tang and J. Kong, *IEEE Trans. Dielectr. Electr. Insul.*, 2017, **24**, 784–790; (*d*) J. Gu, C. Liang, X. Zhao, B. Gan, H. Qiu, Y. Guo, X. Yang, Q. Zhang and D. Wang, *Compos. Sci. Technol.*, 2017, **139**, 83–89; (*e*) J. Gu, X. Yang, Z. Lv, N. Li, C. Liang and Q. Zhang, *Int. J. Heat Mass Transfer*, 2016, **92**, 15–22.
4 F. Ren, G. Zhu, P. Ren, K. Wang, X. Cui and X. Yan, *Appl. Surf. Sci.*, 2015, **351**, 40–47.
5 K. Liang, G. Li, H. Toghiani, J. Koo and C. U. Pittman, *Chem. Mater.*, 2006, **18**, 301–312.
6 J. Ajaja and F. Barthelat, *Composites Part B-Eng.*, 2016, **90**, 523–529.
7 (*a*) C. Alippi, *CAAI Transactions on Intelligence Technology*, 2016, **1**, 1–3; (*b*) X. Sun, J. E. De León, C. Ma, X. Tan and M. Kessler, *Compos. Sci. Technol.*, 2012, **72**, 1692–1696; (*c*) H. Jin, Q. Chen, Z. Chen, Y. Hu and J. Zhang, *CAAI Transactions on Intelligence Technology*, 2016, **1**, 104–113; (*d*) X. Zhang, H. Gao, M. Guo, G. Li, Y. Liu and D. Li, *CAAI Transactions on Intelligence Technology*, 2016, **1**, 4–13.
8 (*a*) Y. Wang, G. Wu, K. Kou, C. Pan and A. Feng, *J. Mater. Sci.: Mater. Electron.*, 2016, **27**, 8279–8287; (*b*) Z. Sun, L. Zhang, F. Dang, Y. Liu, Z. Fei, Q. Shao, H. Lin, J. Guo, L. Xiang, N. Yerra and Z. Guo, *CrystEngComm*, 2017, DOI: 10.1039/C7CE00279C.
9 S. Ohashi, V. Pandey, C. R. Arza, P. Froimowicz and H. Ishida, *Polym. Chem.*, 2016, **7**, 2245–2252.
10 Y. Ye, L. Yuan, G. Liang and A. Gu, *RSC Adv.*, 2016, **6**, 49436–49447.
11 X. Gu, Z. Zhang, L. Yuan, G. Liang and A. Gu, *Chem. Eng. J.*, 2016, **15**, 214–224.
12 Y. Tang, J. Kong, J. Gu and G. Liang, *Polym. Plast. Technol. Eng.*, 2009, **48**, 359–366.
13 L. Zheng, G. Liang, A. Gu, L. Yuan and Q. Guan, *J. Mater. Chem. C*, 2016, **4**, 10654–10663.
14 A. Toldy, Á. Szlancsik and B. Szolnoki, *Polym. Degrad. Stabil.*, 2016, **128**, 29–38.
15 V. Bershtein, A. Fainleib, D. Kirilenko, P. Yakushev, K. Gusakova, N. Lavrenyuk and V. Ryzhov, *Polymer*, 2016, **103**, 36–40.
16 J. Gu, S. Xu, Y. Tang, Z. Lv, C. Liang and X. Meng, *RSC Adv.*, 2015, **5**, 37768–37773.
17 D. Zhuo, A. Gu, Y. Wang, G. Liang, J.-T. Hu, L. Yuan and W. Yao, *Polym. Adv. Technol.*, 2012, **23**, 1121–1128.

18 Z. Zhang, G. Liang, X. Wang, S. Adhikari and J. Pei, *High Perform. Polym.*, 2013, **25**, 427–435.
19 J. Hu, A. Gu, G. Liang, D. Zhuo and L. Yuan, *J. Appl. Polym. Sci.*, 2012, **126**, 205–215.
20 J.-Y. Shieh, S.-P. Yang and C.-S. Wang, *J. Appl. Polym. Sci.*, 2005, **95**, 369–379.
21 J.-Y. Shieh, S.-P. Yang, M.-F. Wu and C.-S. Wang, *J. Polym. Sci., Part A: Polym. Chem.*, 2004, **42**, 2589–2600.
22 J. W. Jung, J. W. Jo, C. C. Chueh, F. Liu, W. H. Jo, T. P. Russell and A. K. Jen, *Adv. Mater.*, 2015, **27**, 3310–3317.
23 B. C. Worley, R. T. Haws, P. J. Rossky and A. Dodabalapur, *J. Phys. Chem. C*, 2016, **120**, 12909–12916.
24 V. S. D. Voet, G. ten Brinke and K. Loos, *J. Polym. Sci. Part A: Polym. Chem.*, 2014, **52**, 2861–2877.
25 A. C. Cooper, I. N. Fleming, S. M. Phyu and T. A. Smith, *J. Cancer Res. Clin. Oncol.*, 2015, **141**, 1523–1532.
26 T.-Y. Lo, Y.-J. Wang, D.-M. Liu and W.-T. Whang, *J. Polym. Res.*, 2015, **22**, 1.
27 A. Vitale, R. Bongiovanni and B. Ameduri, *Chem. Rev.*, 2015, **115**, 8835–8866.
28 J. M. Park, J. H. Jeon, Y. H. Lee, D. J. Lee, H. Park, H. H. Chun and H. D. Kim, *Polym. Bull.*, 2015, **72**, 1921–1936.
29 Y. Guo, W. Liu and Z. Yan, *J. Macromol. Sci. A*, 2015, **52**, 838–846.
30 S. Tian, J. Sun, K. Jin, J. Wang, F. He, S. Zheng and Q. Fang, *ACS Appl. Mater. Inter.*, 2014, **6**, 20437–20443.
31 A. T. Shaver, K. Yin, H. Borjigin, W. Zhang, S. R. Choudhury, E. Baer, S. J. Mecham, J. S. Riffle and J. E. McGrath, *Polymer*, 2016, **83**, 199–204.
32 J. Zhou, L. Fang, J. Wang, J. Sun, K. Jin and Q. Fang, *Polym. Chem.*, 2016, **7**, 4313–4316.
33 L. Tao, H. Yang, J. Liu, L. Fan and S. Yang, *Polymer*, 2009, **50**, 6009–6018.
34 Z. Tao, S. Yang, Z. Ge, J. Chen and L. Fan, *Eur. Polym. J.*, 2007, **43**, 550–560.
35 J. Y. Wang, S. Y. Yang, Y. L. Huang, H. W. Tien, W. K. Chin, C. C. M. Ma and W. J. Shu, *J. Appl. Polym. Sci.*, 2012, **124**, 2615–2624.
36 M. S. Shields and M. J. Reagin, *Appl. Environ. Microb.*, 1992, **58**, 3977–3983.
37 S. Srivastava, K. Bhandari, G. Shankar, H. K. Singh and A. K. Saxena, *Med. Chem. Res.*, 2004, **13**, 631–642.
38 J. T. Kindt and C. A. Schmuttenmaer, *J. Phys. Chem. C.*, 1996, **100**, 10373–10379.
39 Z. Huang, *Preparation of Low Dielectric Constant Polyimide/Pure Silica Zeolite Hybrid Films*, PhD Dissertation, South China University of Technology, 2013.
40 F. Zheng, Y. Zhang, J. Xia, C. Xiao and Z. An, *J. Appl. Phys.*, 2009, **106**, 064105.
41 A. Nagai, A. Takahashi, M. Suzuki and A. Mukoh, *J. Appl. Polym. Sci.*, 1992, **44**, 159–164.
42 J. Gu, Z. Lv, Y. Wu, Y. Guo, L. Tian, H. Qiu, W. Li and Q. Zhang, *Composites Part A-Appl. S.*, 2017, **94**, 209–216.
43 X. Dong, Z. Zhang, L. Yuan, G. Liang and A. Gu, *RSC Adv.*, 2016, **6**, 40962–40969.
44 L. Yuan, G. Liang and A. Gu, *Polym. Degrad. Stabil.*, 2011, **96**, 84–90.
45 F. Chen, L. Yuan, A. Gu, C. Lin and G. Liang, *Polym. Eng. Sci.*, 2013, **53**, 1871–1877.
46 Y. Tu, R. Yu, J. Duan and L. Hu, *Iran. Polym. J.*, 2016, **25**, 863–873.
47 Z. Zhang, J. Pei, G. Liang and L. Yuan, *J. Appl. Polym. Sci.*, 2011, **121**, 1004–1012.
48 H.-J. Hwang, J.-Y. Shieh, C.-H. Li and C.-S. Wang, *J. Appl. Polym. Sci.*, 2007, **103**, 1942–1951.
49 Y. Wang, Y. Yuan, Y. Zhao, S. Liu and J. Zhao, *High Perform. Polym.*, 2017, **29**, 94–103.

